Facile preparation of nanofibrillar networks of “ureido-chitin” containing chelating functional groups: ureido and amine

Kathirvel Ganesan,* Markus Heyer, Lorenz Ratke and Barbara Milow

Department of Aerogels, Institute of Materials Research, German Aerospace Center, Linder Hoehe, 51147 Cologne, Germany.

Abstract: Aerogels of polysaccharide with chelating functions can be useful as supports in many applications because of their hosting property. We demonstrate a facile method for the preparation of aerogels of chitosan derivative, “ureido-chitin” containing ureido functional group. The nanofibrillar networks of “ureido-chitin” were produced by the nucleophilic addition of amine groups of chitosan with *in situ* prepared isocyanic acid. The presence of ureido functional groups was confirmed by FT-IR, solid state CP-MAS ^{13}C and ^{15}N NMR. No crosslinking of molecular chains was observed. The maximum degree of ureido functional groups was estimated to be about 66 %. Characterization by powder XRD confirmed that the polymer chains self-assembled in a way how the chitin polymers orient themselves in a highly ordered crystalline structure. The nanofibrillar networks showed no solubility under aqueous acidic and alkaline conditions. Bio-based hosting materials of this kind with two different hosting functional groups: ureido and amine can be potentially utilized for wide applications in aqueous medium including filters, catalysis and biomedicine.

1. Introduction

Aerogels of polysaccharides with chelating functional groups such as -NH_2, -OSO_3H, -COOH have attracted great interest in recent research due to the fact that they can act as hosts in applications where high chemical affinity to guest atoms/molecules is required. Offering the host-guest chemical relation, aerogels of polysaccharide materials with chelating functional groups can be employed as carrier/supporting systems in many applications including catalysis, separation and sensing techniques and biomedicines.[1] Through our ongoing research work exploring the methods to prepare aerogels of polysaccharides with chelating functions,[2] we have accomplished that it is essential to develop new aerogel materials with a desirable feature such as sustain under acidic and alkaline medium. The new sustainable feature of aerogels should offer the materials being potentially used again after their function in applications. Recent reports[3] of nanomaterials showed the development of sustainable features with the high efficiency of hosting property which have been achieved only after chemically modifying the available functional groups of polysaccharides. Therefore, taking advantage of the well-defined chelating functionality and carefully synthesizing chemically modified porous structure make it possible to bring the excellent hosting properties with complete control on the nanofibrillar network.

Chitosan is one of the important derivatives of chitin. Because of its renewable resource, biocompatibility, biodegradability and antimicrobial properties, chitosan, chitin and their derivatives are widely used in many applications including biomedicine, catalysis, agriculture and purification and separation techniques.[4] Highly porous chitosan-based materials can offer potential chelating functional properties. Recently, Wang et al.[3d] demonstrated that highly porous chitosan foams with chelating amine functional groups can be a promising adsorbent materials for anionic dyes in which the elution of dyes have been accomplished with alkaline treatment of the foams. Yang et al.[3b] reported the reusable of hybrid (cellulose and chitosan-based) foams for the removal of cationic

dyes. In this case the dye molecules were desorbed by treating the hybrid foams in 0.1 M HCl, followed by washing with 0.1 M NaOH solution. Both of these literatures[3b, 3d] proved the excellent functional properties of foams for many cycles.

Water soluble property of chitosan under mild acidic condition offers the opportunity to do the chemical modifications in environment friendly atmosphere. Mostly, chemically modified chitosan aerogels were prepared by Schiff-base reaction where the nucleophilic amine groups react with different aldehydes (glutaraldehyde, glyoxal and formaldehyde).[1h, 5] These chitosan aerogels, after supercritical drying, displayed to have highly porous nanostructure with surface area in the range 400-485 m^2/g. Water soluble derivative of chitosan aerogel was reported[6] by treating acidic aqueous solution of chitosan with L-glutamic acid. Chitin aerogels have been prepared from chitosan by the acetylation of amine functional groups of chitosan in an acidic aqueous solution using acetic anhydride as an acetylating agent.[7] Ureido derivative of chitosan was reported in recent literature.[8] Jing et. al.[8b] have demonstrated that ureido-conjugated chitosan/tripoly phosphate nanoparticles can be used as potential drug loading material for effective therapy of *Helicobacter Pyroli* infection.

Herewith, we report a facile method to synthesize aerogels of chitosan derivative ("ureido-chitin"; UC) containing ureido and amino functional groups. Ureido functional group is a well-known neutral organic receptor especially for complexing anions and cations through hydrogen and coordinate bonding.[9] Chitosan and urea were treated in an aqueous acidic medium yielding the hydrogels of UC containing ureido functional groups. After washing and drying, the results have proven that the aerogel materials have two different chelating functional groups: 66 % of ureido function and 33 % of amine function. We strongly believe that the presence of potential chelating functional groups (ureido and amine) on the nanofibrillar networks of aerogels with a mesoporous function can be acting as host for the wide applications including filters, catalysis and biomedicine.

2. Experimental Section

2.1. Materials

Chitosan (shrimp shell grade; ≥75% deacetylated), acetic acid and urea were obtained from Sigma Aldrich. Sodium hydroxide was obtained from Merck. For all the syntheses and washing processes deionized water was employed. Ethanol was employed for solvent exchange process. Supercritical drying was carried out in an autoclave using pure carbon dioxide, following the procedure reported by Hoepfner et al.[15]

2.2. Characterization techniques

The products were characterized by envelope density measurement (Micromeritics – GeoPyc 1360), skeletal density (Micromeritics – Accupyc II 1340; Gas Pycnometer – Helium), BET nitrogen adsorption–desorption isotherm analysis (Micromeritics – Tristar II 3020), Fourier transform infrared spectroscopy (FTIR; Bruker-Tensor 27 instrument), scanning electron microscopy (SEM: Merlin – Carl Zeiss Microscope; gold sputtered samples) and transmission electron microscopy (TEM: Philips Tecnai F30 with CCD camera). The XRD measurements of monolithic and powder samples were performed on a Bruker D8 DISCOVER diffractometer using Cu-Kα radiation (λ = 1.54 Å). Solid state NMR analyses were carried out with a Bruker 400 WB spectrometer operating at a proton frequency of 400.13 MHz. NMR spectra were acquired with cp and proton decoupled sp pulse sequences under the following conditions: ^{13}C NMR frequency = 100.48 MHz, π/2 pulse 3.7 μs, decoupling length 6.3

µs, recycle delay: 60 s, 2000 scans. ^{15}N NMR frequency = 40.34 MHz, π/2 pulse 3.6µs, contact time 5 ms, decoupling length 6.3 µs, recycle delay: 10 s, 20000 scans. Samples were packed in 4 mm zirconia rotors which were spun at 8 kHz under air flow. Adamantane (δ-CH_2 group at 38.5 ppm) and glycine (δ-NH_2 at 32.4ppm) were used as external secondary references. The elements carbon, hydrogen and nitrogen were determined by standard combustion analysis with an EA 1110 (CE Instruments) instrument. To determine the weight average molecular weight, gel permeation chromatography (GPC) analyses were carried out at 40°C using Agilent 1200 system with an UV detector (Agilent 1200 VWD), a refractive index detector (Agilent 1200 RI) and a multi angle laser light scattering detector (MALLS; Wyatt EOS). The eluting solvent was 0.1% TFA, 0.1M NaCl, 0.01% NaN_3 in water (HPLC grade), which was degassed by Agilent system. The flow rate was 1mL/min. The samples were dissolved by adding 4 mL of eluting aqueous solvent to 25 mg of sample together with 1% of v/v HCl. The samples were injected via an Agilent 1260 Auto-sampler. Calibration was achieved using PEG standards of narrow molecular weight distribution (Polymer Standards Service PSS). Thermogravimetric analysis was performed in Netzsch TG 209 F1 instrument (dynamic argon atmosphere; argon flow rate 20 mL/min; heating rate 10 K/min; open alumina crucible).

2.3. Synthesis of UC aerogels containing ureido functional groups

The powder of chitosan (~99% of deacetylated) was prepared from commercial chitosan powder according to a method reported in the literature.[12] A solution of ~99% of deacetylated chitosan (2 wt%) was prepared by dissolving the chitosan in an aqueous acetic acid in the presence of urea. The molar concentration of acetic acid was 0.3M. And the concentration of urea was varied from 1 to 12 molar equivalents with respect to acetic acid concentration. The ratios of acetic acid/Urea were 1:1, 1:2, 1:3, 1:6, 1:9 and 1:12. The clear solution was filtered through Whatman filter paper in order to remove any dust particles. The reaction mixture was taken in a sealable container, purged with nitrogen gas for 15 minutes, tightly closed and warmed in an oven at 70 °C until gelation occurs. During gelation, the pH of the reaction mixture was raised from 3-3.2 to 5.2-5.4 due to the decomposition of urea and the production of ammonia. After gelation, the gel medium was washed with NaOH solution (1M) in order to neutralize the nanofiber network and then several times with water until the supernatant becomes neutral. Finally the aqueous solvent medium was exchanged to ethanol. After supercritical drying (at the temperature of 45 °C and above the critical pressure of CO_2, ca. 95 bar), the aerogels were obtained.

3. Results and Discussion

3.1. Synthesis of aerogels of chitosan derivative

We have established a facile method to synthesize the aerogels of chitosan derivative having ureido functional groups which are named “ureido-chitin” and abbreviated as UC hereafter. The formation of aerogel from chitosan and urea mixture in an aqueous acidic solution is illustrated in Figure 1.

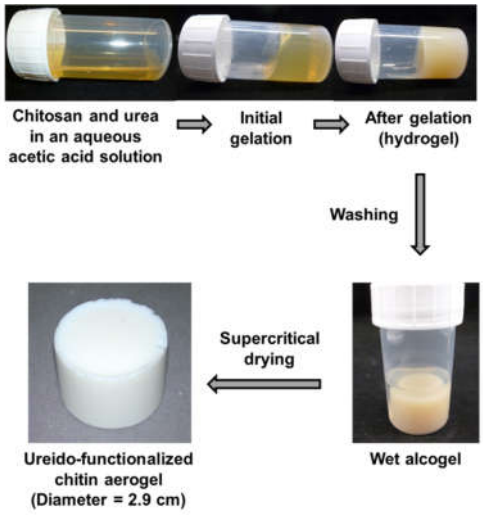

Figure 1. Image illustrating the stepwise process for the preparation of UC.

A homogeneous clear aqueous solution of a mixture of chitosan, urea and acetic acid was heated at or above 70 °C in an oven until gelation. The initial light yellow clear solution became translucent during gel initiation. The aerogels can also be prepared from this initial gelation point but the samples were deformed from its original shape (see supplementary information, Figure SI-1). It may be due to the incomplete network formation. Further heating turned the gel to become opaque (Fig. 1) and there was no movement of the gel while tilting the container. The reaction was stopped at this point to avoid formation of any side products. After washing hydrogel with NaOH solution, neutralizing with water, exchanging the aqueous medium with alcohol and supercritical drying, the pure aerogels (UC) were obtained. The samples were white in color, intact in shape and no deformation was observed during the drying process (Fig. 1).

3.2. Reaction mechanism

The schematic diagram of the possible reaction mechanism is shown in Scheme 1. Isocyanic acid is produced by the decomposition of urea at or above 70 °C which is volatile in solution and further it can readily decompose into ammonia and carbon dioxide in an aqueous medium. The acid medium can temporarily stabilize the *in situ* produced isocyanic acid. This is a key step in the reaction where the acid-stabilized isocyanic acid can undergo addition reaction with the amine groups of chitosan. Preferably, the nucleophilic addition reaction can occur with the electron deficient carbonyl group from isocyanic acid (indicated by arrow mark) which is more electrophilic than carbonyl group from acetic acid. As a result, after gelation, the aerogels (UC) were produced. In the absence of urea, there was no gelation. Changing the acid concentration from 0.3 to 0.5M at the same time keeping the molar ratio between urea and acid did not affect the gelation time. Therefore the presence of urea and its decomposition product, isocyanic acid play a pivotal role in the production of UC.

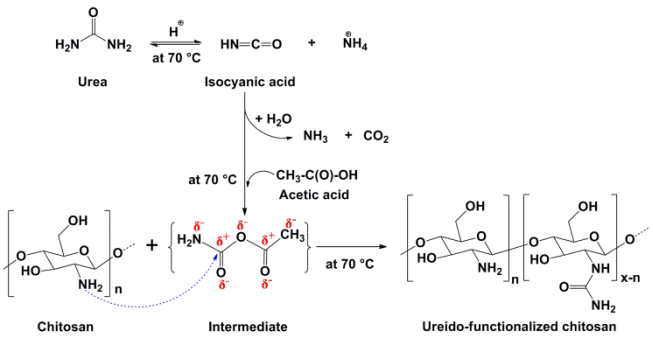

Scheme 1. Proposed reaction mechanism illustrating the formation of UC.

3.3. Gelation time

The gelation time is dependent on the molar ratio of the urea and acetic acid, the decomposition temperature of urea and the availability of isocyanic acid in the reaction mixture. If the molar ratio of urea to acetic acid is ≤2, the gelation time is more than 65 hours at 70 °C (see Fig. 2) and syneresis and large volume shrinkage occurs. Using the molar ratio of urea to acetic acid ≥3, it is possible to produce the dull yellow color hydrogels showing no syneresis. In this case, the gelation time is drastically decreased. Particularly, after the molar ratio ≥6, the curve stretches to a good linear fit (Fig. 2, blue line). It indicates that there is a sufficient amount of isocyanic acid available for the nucleophilic addition reaction. When the reaction temperature is increased from 70 to 80°C, the gelation time drastically decreases. For instance, the gelation time is 4 times decreased (i.e. ~32 hours to ~8 hours) for the mixture with a molar ratio of urea to acetic acid 3. Regardless of the difference in gelation time, we used the molar ratio of urea to acetic acid ≥3 in order to obtain the highly porous material.

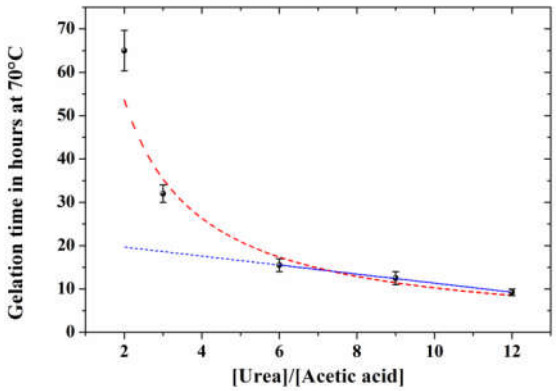

Figure 2. Gelation time at 70 °C with respect to the molar ratio of urea to acetic acid.

3.4. Physical properties of aerogels

The physical properties of aerogels are summarized in Table 1. The aerogels showed volume shrinkage during the washing and drying processes. Varying the molar ratio of urea to acetic acid from 3 to 12 showed almost no difference in volume shrinkage of alcogels and aerogels. The measurement of the volume after washing with NaOH solution, water and ethanol gave volume shrinkage of alcogels that was in average about 18 vol%. The supercritical drying process reduced further about 31 vol% of gel from the volume of alcogels. Considering the total shrinkage from the volume of hydrogel, after washing and drying processes, about 51 vol% was obtained as aerogels.

But, at the molar ratio of urea to acetic acid 2, only about 26 vol% of sample was recovered as aerogels (see Table 1). It may be due to decrease in the gel strength that is directly related to the temperature, pH and gelation time.

Table 1. Physical properties of aerogels (UC). The average values of at least two measurements were shown.

[Urea]/[Acetic acid]	Total volume shrinkage (%)	Envelope density, ρ_e (g/L)	BET surface area (m^2/g)	Porosity (%)
2	74.0 ± 0.8	170	172	88.7
3	50.0 ± 0.7	78	299	94.8
6	47.9 ± 0.7	71	310	95.3
9	49.9 ± 1	73	306	95.1
12	48.5 ± 1.2	71	305	95.3

The specific surface area of aerogels was analyzed from nitrogen adsorption-desorption isotherms. Type IV isotherm, according to IUPAC nomenclature, was observed for all samples (see an example of isotherm linear plot in supplementary information, Figure SI-2). The specific surface area (S_m) value was about 305 m^2/g if the molar ratio of urea to acetic acid was ≥3 whereas the surface area was 172 m^2/g if the molar ratio of urea to acid was 2. This decrease in surface area can be attributed to the high volume shrinkage and collapse of network.

The envelope density of aerogels of UC exhibited significantly low values about 71 to 78 g/L for the samples prepared from the molar ratio of urea to acid ≥3 comparing with the samples prepared from urea to acid molar ratio of 2. The skeletal density (ρ_s) of aerogels of UC was measured to be in average about 1.5 kg/L which can be comparable to chitin nanowhisker aerogels.[10]

$$\text{Porosity} = 100 \times (1-(\rho_e/\rho_s)) \quad (1)$$

The porosity of aerogels was calculated from the equation (1). The results showed that the aerogels prepared with urea to acetic acid ratio ≥3 has very high porosity of ~95% in comparison with the samples prepared with urea to acetic acid ratio 2 (about ~89 %).

The average nanofiber diameter can be estimated from the equation (2) using the relationships of the specific surface area (S_m) and skeletal density (ρ_s) with fiber diameter (D).

$$D = 4/(\rho_s.S_m) \quad (2)$$

Using the above values (Table 1), we calculate an average fiber diameter of *ca*. 8.8 nm for the aerogels obtained using the molar ratio of urea to acid ≥3.

3.5. Analysis of microstructures of UC aerogels

Scanning electron microscopy (SEM) images of aerogels are shown in Figure 3. The fractured surface of the aerogels exhibited the interconnected nanofibrillar structure similar to cellulose and other

polysaccharide aerogels. The aerogels prepared with a molar ratio of urea to acetic acid 2 showed a densely packed nanofibrillar network with a fiber thickness of 15 to 20 nm and the nanofibers were closely packed (Fig. 3a). It may be due to massive volume shrinkage of the bulk material. On the contrary, the aerogels obtained from higher molar ratio of urea to acetic acid ≥3 yielded almost similar microstructure with a fiber thickness of 8 to 12 nm. The data suggests that the usage of higher molar concentration of urea with respect to the concentration of acid ≥3 can provide interconnected nanofibers with high porosity, high specific surface area, low density, less volume shrinkage and short gelation time.

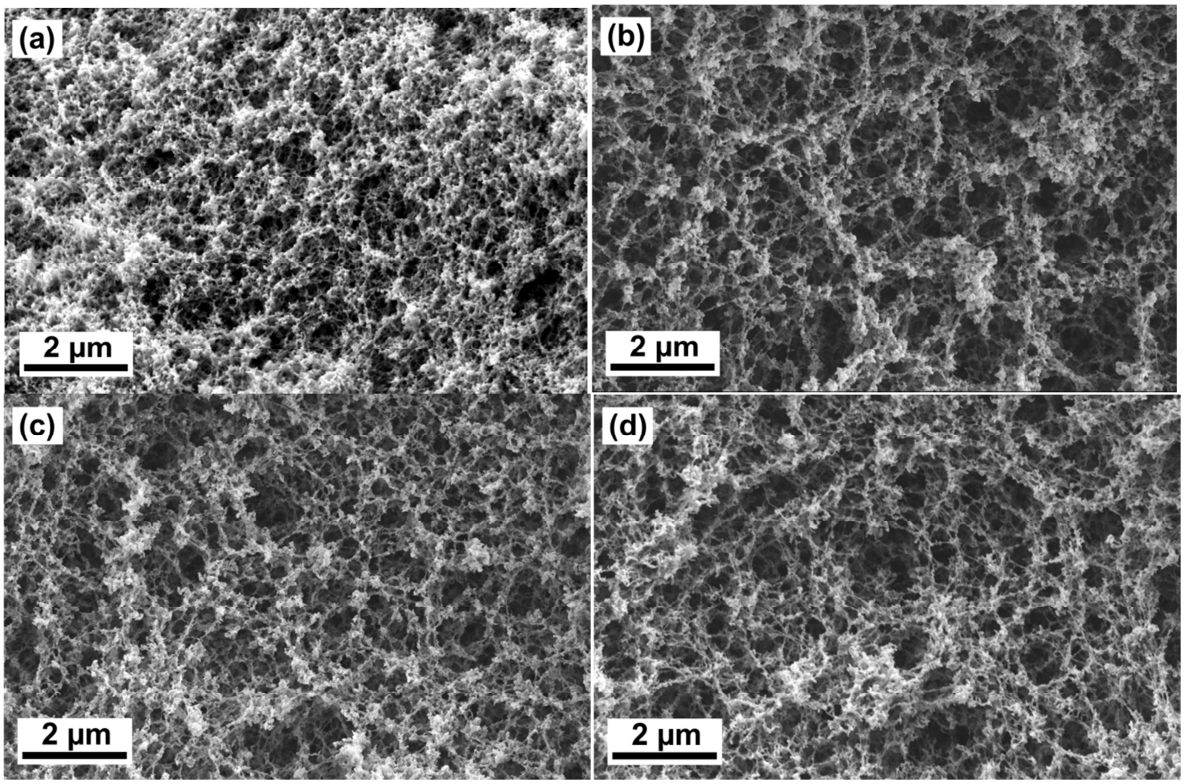

Figure 3. Comparison of the scanning electron microscopy images of aerogels of UC prepared with a molar ratio of urea to acetic acid: (a) 2, (b) 3, (c) 6 and (d) 12.

The microstructure was also analyzed using transmission electron microscopy (TEM). Figure 4 shows the TEM micrographs of aerogels prepared with a molar ratio of urea to acetic acid 6. It exhibits the interconnected nanofibrillar structure which is not deviating from the observations of SEM image analysis (see Figure 3). The higher magnification image displays the fiber thickness of about 10.9 nm.

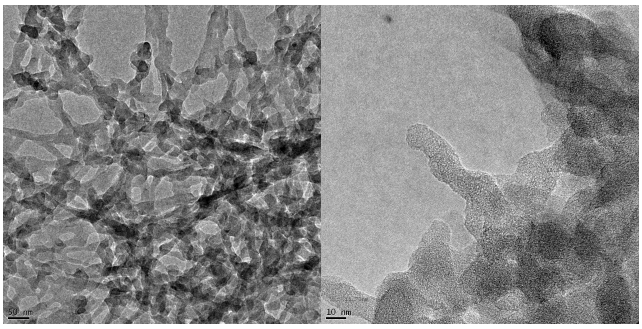

Figure 4. Transmission electron microscopic images of UC aerogels prepared with a molar ratio of urea to acetic acid 6 (scale bar: left 50 nm and right 10 nm).

3.6. Analysis of degree of reaction

The solid state CP-MAS ^{13}C NMR of aerogels was compared with chitosan powder (Fig. 5). The assignment of the peak positions for the carbon atoms in the polysaccharide backbone was done according to the literature.[11] The peak at 162 ppm was assigned to the carbonyl functional group of ureido (–NH-C(O)-NH_2) in UC aerogel. The integration of the peaks was carried out in order to calculate the quantitative amount of the presence of ureido functional groups. In specific, it was quantitatively evaluated from the relative integral of carbonyl (-NH-C(O)-NH_2) group comparing to the carbon integrals (C3, C4 and C5) in the polysaccharide backbone. As the kinetics of cross-polarization should not be the same for each carbon atoms in a monomer unit,[11] a systematic error of at least 5 % can be considered for this quantitative evaluation. The integration values are shown in Table 2. It revealed that the degree of ureido functional group was 66 %.

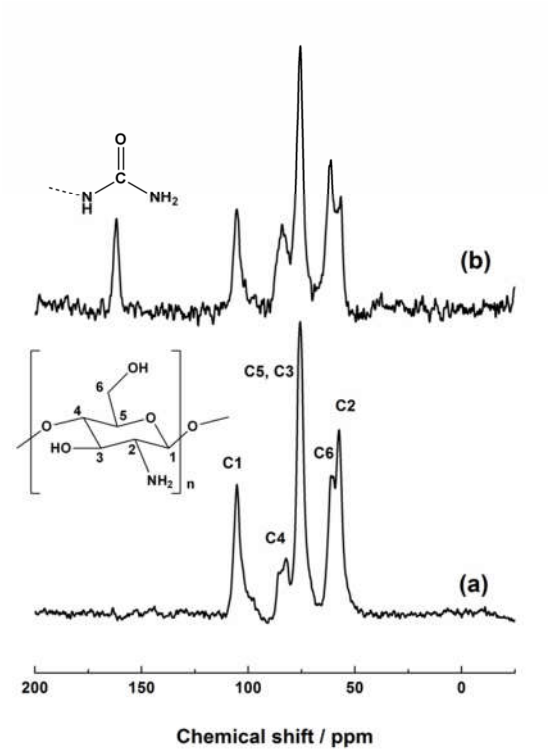

Figure 5. Comparison of solid state CP-MAS ^{13}C NMR of chitosan (a) and UC aerogel (b).

Table 2. The solid state CP-MAS ^{13}C NMR resonance peaks with the assignment of functional groups and the integration values.

The peak position, δ (ppm)	Assignment of functional groups	Integration value
162	-C(O)-	0.66
105-104	C1	0.94
83.1 and 75.6	C5, C4 and C3	3
61.3 and 57.7	C6 and C2	2.27

To do the qualitative analyses, we have performed the solid state CP-MAS ^{15}N NMR. Figure 6 shows the comparison spectra of ^{15}N NMR of chitosan and UC. The peak at 23 ppm was assigned to the –NH_2 group of chitosan. For the UC aerogel, two peaks were observed in the down field: 76.3 and 86.9 ppm indicating the presence of non-equivalent nitrogen atoms which were assigned to -C(O)-NH_2 and -NH-C(O) respectively. The careful analysis of area under the peaks showed nearly same value. The full width at half maximum (FWHM) was calculated for the peak at 76.3 ppm that was noticeably broader (FWHM = 11.4 ppm) but showing lower intensity than the peak at 86.9 ppm(FWHM = 8.5 ppm). We assume that the peak broadness at 76.3 ppm may be due to the mobility of –C(O)-NH_2 bond. These qualitative analyses confirm that the obtained aerogel products after gelation have ureido functional groups (-NH-C(O)-NH_2).

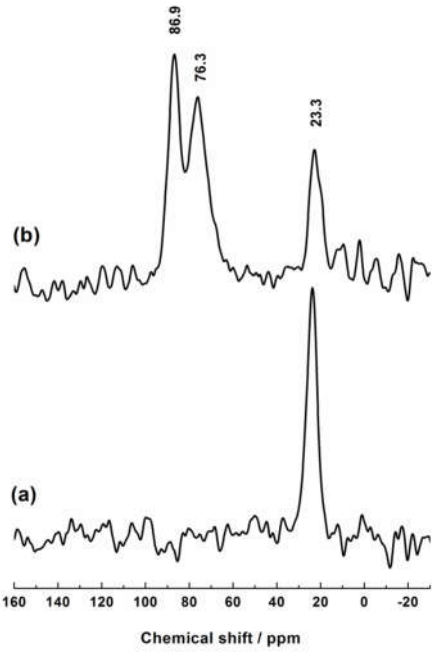

Figure 6. Comparison of solid state CP-MAS ^{15}N NMR of chitosan (a) and aerogel of UC (b).

3.7. Crosslinking behaviour

The samples were also examined for crosslinking possibilities. For this purpose, after gelation ([urea]/[acetic acid] = 6), the gel was warmed at 70 °C for 30 hours i.e., about 2 times longer duration than the original gelation period. The CP-MAS ^{15}N NMR data of this product is shown in supplementary information (Figure SI-3). The spectrum exhibited only two peaks: 76.4 and 87.4 ppm. The area under the peak at 87.4 ppm was about three times higher than the peak at 76.4 ppm which was still broader and having very low intensity. Although CP-MAS ^{15}N NMR is considered only for qualitative analysis, not a quantitative, this difference in peak intensity and the disappearance of –NH_2 peak of chitosan indicate the formation of crosslinking product (-NH-C(O)-NH-) if the hydrogels are still warmed after gelation.

3.8. Molecular weight analysis

The weight average molecular weight (Mw) was determined by means of Gel Permeation Chromatography (GPC) analyses (Figure 7). For this analysis, the water soluble form (under acidic

condition) of the ureido-functionalized product was taken in to account. That is, at 3.25/4 of the gelation time or just before initial gelation occurred; the reaction mixture was collected, neutralized and washed with water and ethanol. The vacuum dried product was dissolved and eluted through the GPC. The results exhibited that weight average molecular weight of ureido-functionalized product had obviously lower value than chitosan (99% deacetylated) (see Table 3). It may be due to the heating process of the solution at 70°C. This analysis confirms that the product has the linear chain structure of ureido-functionalized chitosan or no crosslinking occurs during gelation, supporting the data of CP-MAS ^{15}N NMR. It is believed that the weight average molecular weight could not have major change in molecular weight during the process of initial gelation and gelation, as it is the step of solid network formation.

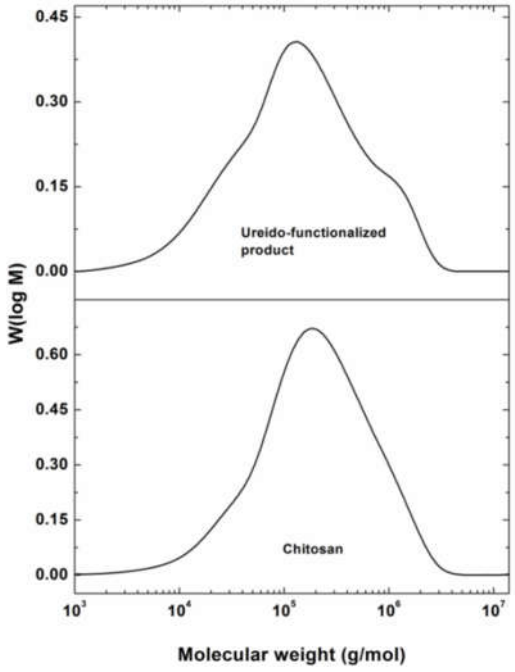

Figure 7. Molecular weight distribution of chitosan and ureido-functionalized product before initial gelation ([Urea]/[acetic acid] = 6; at 70°C).

Table 3. Weight average molecular weight (Mw) and polydispersity index of polymers: chitosan (99% deacetylated) and ureido-functionalized product at 3.25/4 of the gelation time ([Urea]/[acetic acid] = 6; at 70°C).

Sample	Mw (g/mol)	Polydispersity
Chitosan (99% deacetylated)	366720	4.74
Ureido-functionalized product	317540	5.95

3.9. Elemental analysis

The elemental analysis of UC aerogel was found to be in average about: C 41.15, H 6.46, N 11.85, O 40.25. This has an N/C ratio of 0.288 which is higher than the N/C ratio of chitosan (0.194 for fully deacetylated). The calculated degree of addition reaction or the quantitative amount of ureido functional group was ca. 64 %. This data is in very good agreement with the CP-MAS ^{13}C NMR data.

3.10. Crystalline phases of ureido-functionalized products

The reaction process and the change in crystalline phase were followed by collecting the intermediate products in different intervals from the reaction medium until the gelation occurred. For that, before gel formation, the solutions were collected, neutralized and washed with water and ethanol. The wet powder was then dried under vacuum at 60 °C. The samples were analysed by powder XRD and FTIR and compared the data with aerogel of UC. The crystallinity of the products changes during the formation of ureido derivatives which was confirmed by powder XRD (Fig. 8). The change in diffraction pattern was observed when the reaction time increases ≥3/4 of the gelation time. The intense XRD pattern at 20.5 was assigned to ureido-functionalized chitosan derivative, (no gelation; Fig. 8a) which shifted to 19.5 when the gelation occurred (Fig. 8e). There were two more new peaks arising at 9.6 and 26.3 during gelation (Fig. 8d and 8e). The observed change in crystallinity can be caused due to the change in chemical environment and the difference in oriented assembly of polymer chains. Interestingly, comparing the diffraction pattern of UC with native chitin (Fig. 8e and 8f), we have concluded that the polymer chains of UC self-assemble themselves and adapt the oriented crystalline packing of native chitin. For this reason, after gelation, the obtained aerogel products are named “ureido-chitin” (UC).

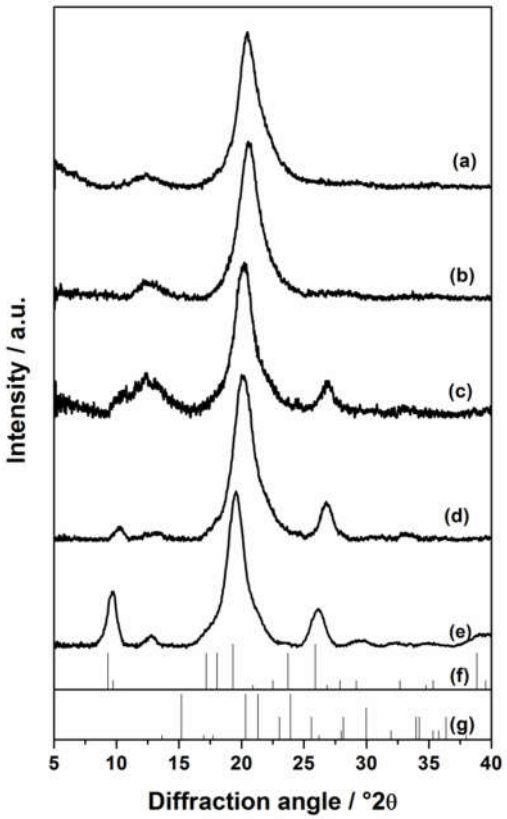

Figure 8. Powder X-ray diffraction pattern showing the change in crystallinity of the chitosan polymer during gelation. (a) ¼ of the gelation time, (b) ½ of the gelation time, (c) ¾ of the gelation time, (d) initial gelation (refer Figure 1) and (e) aerogel of UC. (f) and (g) are the reference diffraction patterns

of chitin (PDF number = 00-035-1974) and chitosan (PDF number = 00-039-1894) respectively which are obtained from the International Center for Diffraction Data.

3.11. Anaysis of FTIR data

Figure 9 shows the FTIR data illustrating the change in vibrational bands of chitosan during gelation. The IR spectrum of chitosan from shrimp shell (SS) was analysed to have ~99 % of NH_2 functional groups.[12] The assignment of vibrational bands for chitosan, UC and native chitin were shown in Table SI-1. The shoulder peak at 1655 cm^{-1} was assigned for about 1 % of –NH-C(O)-CH_3 group. The vibrational band at 1600 cm^{-1} was assigned for –NH_2 group, indicated by a vertical dotted line. This spectrum of chitosan was compared with the spectra of the samples obtained from different intervals until gelation. The formation of ureido-functionalized of chitosan and UC were confirmed by following the vibrational bands of the ureido, –NH-C(O)-NH_2 functional group. By increasing the reaction period, the vibrational band of –NH_2 group gradually disappeared because of the growth of two amide vibrational bands assigning at 1657 cm^{-1} and 1564 cm^{-1}. The absence of vibrational bands of -C=O for ester group in the region between 1700 to 1750 cm^{-1} revealed that the reaction occurred only between -NH_2 group and isocyanic acid intermediate.

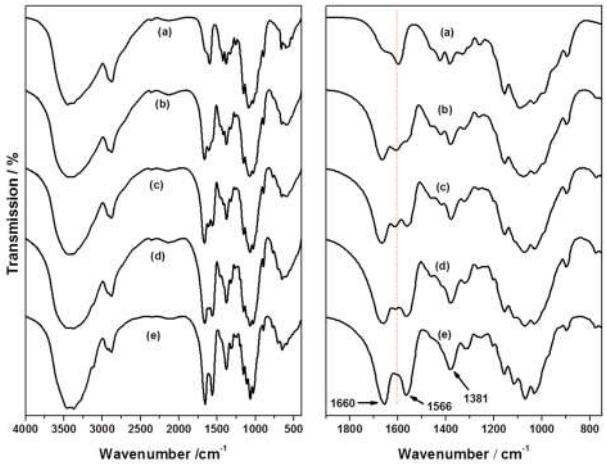

Figure 9. FTIR spectra illustrating the change in vibrational bands of chitosan during gelation: (a) chitosan from shrimp shell, (b) ¼ of the gelation time, (c) ½ of the gelation time, (d) ¾ of the gelation time and (e) aerogel of UC. The expanded plots (1900 to 750 cm^{-1}) of the FTIR spectra are shown on the right side. The vertical dotted line (red) on the right side plot indicates the vibrational band of –NH_2 group at 1597 cm^{-1}.

The FTIR spectra of chitosan (99 %), UC were compared with native chitin (Figure SI-4). In comparison with chitin spectra, the vibrational bands of O6-H and O3-H bonds from UC were observed at lower wavenumbers, 3456 cm^{-1} and 3371 cm^{-1} respectively (see Table SI-1).[13] It indicates that the O6-H and O3-H bonds are very influenced by inter- and intramolecular hydrogen bonding in the presence of ureido-functional groups. Interestingly, the peak at 1423 cm^{-1} ascribed to CH_2 bending in Figure SI-4a disappeared after gelation (see Fig. SI-4) as the vibrational band at 1381 cm^{-1} assigned for C-H bending became broader. In addition, the band at 1092 cm^{-1} assigned for C-O functional group (Fig. 7a) split into two peaks after gelation (1115 and 1069 cm^{-1}). Whereas the band assigned for asymmetric bridge C-O-C stretching had very little effect, about 2 cm^{-1} shifted to upper wavenumber. Although the understanding of the orientation of UC remains to be solved, we can conclude from the

data that these changes in vibrational bands occurred due to the difference in inter- and intramolecular hydrogen bonding and the change in crystallinity during precipitation or gelation.

3.12. Thermogravimetric analysis

The thermal stability and decomposition of aerogel was characterized by thermogravimetric analysis (Figure 10). The first decomposition step until 120 °C corresponds to the loss of adsorbed water molecules. It was estimated that about 4 to 8 % of water molecules were adsorbed on the chitin and chitosan molecules. In the second step of decomposition, the aerogels of UC decomposes at higher temperature, 330 °C than chitosan from shrimp shell (~99% deacetylated, 301 °C). For comparison, native chitin molecules decompose at 344 °C. Therefore the thermogravimetric analysis suggests that the presence of ureido functional groups improve the thermal stability of the polymer chain.

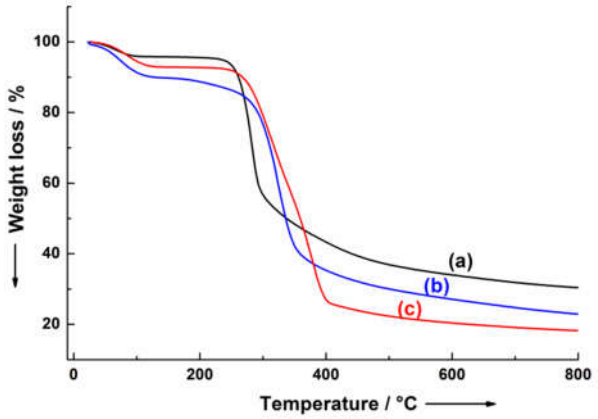

Figure 10. Thermogravimetric analysis of chitosan from shrimp shell (~99 % deacetylated) (a), UC (b) and native chitin from shrimp shell (c).

3.13. Sustainability in aqueous medium

The sustainability of nanofibrillar networks of aerogel at different pH values in an aqueous medium was characterized by following the solvent uptake property while dipping the aerogel in the appropriate solvent for 5 minutes duration. Under aqueous acetic acid medium at pH 3, the aerogels uptake water molecules about 11.6 times higher than the original weight of dry aerogel whereas under alkaline medium, aqueous NaOH at pH 10.5, only 10 times absorption of water was observed. The increase in water uptake under acidic condition may be due to the protonation of unreacted -NH_2 functional group on the surface of the nanofibers. At neutral pH condition, about 9.5 times of water was absorbed. Under these different aqueous medium, the aerogel samples were stable even for longer duration (24 h) and no deformation was observed. This difference in the amount of water uptake was only because of the properties of aerogels: chemical functional groups on the nanofibers, high specific surface area and open porosity of the material. This insoluble behavior of material in acidic and alkaline medium can provide the opportunities to utilize the aerogel as reusable in applications like the reported literature[3b, 3d].

3.14. Mechanical property

Figure 11 shows the compression stress-strain curve of UC aerogel which was prepared with a molar ratio of urea to acetic acid 6. The Young's modulus of UC aerogel was 1.7 MPa and 1 % yield stress was 69 kPa. During compression, the stress-strain curve of UC aerogel showed initially a rapid

increasing elastic regime, after then plastic collapse region and finally densification after 65 % of strain. The plastic collapse region was observed to be not smooth like cellulose aerogels[14]. After 17.5 % of strain, the sample reached the ultimate stress and the stress dropped off but the sample was not completely fractured into pieces. It suggests that the onset of nanofibrils undergo elastic bending (but not folding up continuously like in cellulose aeorgels), then plastic yielding and fracturing.

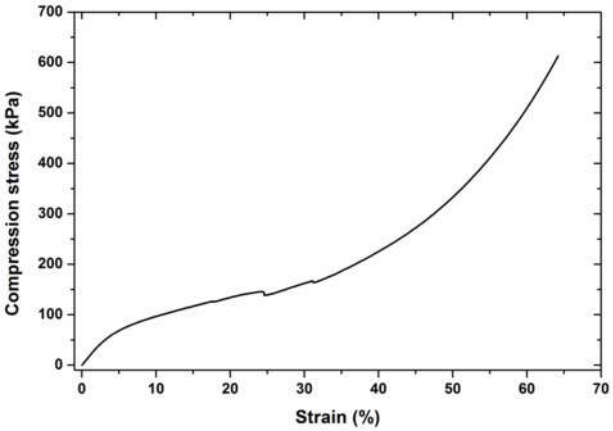

Figure 11. Compression stress-strain curve of UC aerogel.

4. Conclusions

We have demonstrated a facile synthesis method of UC aerogels containing ureido functional groups. In this method urea was used as the source of isocyanic acid which can selectively undergo nucleophilic addition reaction with -NH_2 group in chitosan. By this reaction, the degree of ureido functional groups can be achieved maximum up to 66 % which was confirmed by solid state CP-MAS ^{13}C NMR and elemental analysis. The UC aerogels offer two different chelating functionalities: ureido (neutral) group and amine (polarizable) group. As the experimental evidences are convincing, these aerogels can be used as supporting materials for environmental control system chelating the guest molecules under acidic and alkaline medium.

Acknowledgements

We gratefully thank Dr. Emanuela Callone performing the solid state ^{13}C NMR analyses using the equipment of the “Klaus Müller” NMR Laboratory of the Industrial Engineering Department at the University of Trento. We thank Dr. Matthias Kolbe for his help with scanning electron microscopy and Dr. Alexander Francke for his assistance with powder X-ray diffraction data. We thank center for chemical polymer technology (CPT), DWI-Leibnitz-Institut für Interaktive Materialien e.V. for their assistance in molecular weight determination experiments.

Keywords: Chitosan • Chitin • Gels • Aerogels • Ureido

References:

[1)] aA. Primo, M. Liebel, F. Quignard, *Chem. Mater.* **2009**, *21*, 621-627; bS. Frindy, A. Kadib, M. Lahcini, A. Primo, H. García, *ChemCatChem* **2015**, *7*, 3307-3315; cA. Ricci, L. Bernardi, C. Gioia, S. Vierucci, M. Robitzer, F. Quignard, *Chem. Commun.* **2010**, *46*, 6288-6290; dT. Mehling, I. Smirnova, U. Guenther, R. H. H. Neubert, *J. Non-Cryst. Solids* **2009**, *355*, 2472-2479; eA. Veronovski, Z. Novak, Ž. Knez, *J. Biomater. Sci., Polym. Ed.* **2012**, *23*, 873-886; fC. Garcia-Gonzalez, M. Alnaief, I. Smirnova, *Carbohyd. Polym.* **2011**, *86*, 1425-1438; gC. Gioia, A.

Ricci, L. Bernardi, K. Bourahla, N. Tanchoux, M. Robitzer, F. Quignard, *Eur. J. Org. Chem.* **2013**, *2013*, 588-594; hX. Chang, D. Chen, X. Jiao, *J. Phys. Chem. B* **2008**, *112*, 7721-7725.

[2)] K. Ganesan, L. Ratke, *Soft Matter* **2014**, *10*, 3218-3224.

[3)] aP. S. Barber, S. P. Kelley, C. S. Griggs, S. Wallace, R. D. Rogers, *Green Chem.* **2014**, *16*, 1828-1836; bH. Yang, A. Sheikhi, T. G. M. v. d. Ven, *Langmuir* **2016**, *32*, 11771-11779; cJ. N. Putro, A. Kurniawan, S. Ismadji, Y.-H. Ju, *Environ. Nanotechnol. Monit. Manage.* **2017**, *8*, 134-149; dM. Wang, Y. Ma, Y. Sun, S. Y. Hong, S. K. Lee, B. Yoon, L. Chen, L. Ci, J.-D. Nam, X. Chen, J. Suhr, *Sci. Rep.* **2017**, *7*, 18054.

[4)] aE. Khor, L. Y. Lim, *Biomaterials* **2003**, *24*, 2339-2349; bM. Rinaudo, *Prog. Polym. Sci.* **2006**, *31*, 603-632; cC. K. S. Pillai, W. Paul, C. P. Sharma, *Prog. Polym. Sci.* **2009**, *34*, 641-678; dR. Jayakumar, D. Menon, K. Manzoor, S. V. Nair, H. Tamura, *Carbohyd. Polym.* **2010**, *82*, 227-232; eV. S. Yeul, S. S. Rayalu, *J. Polym. Environ.* **2013**, *21*, 606-614; fM. N. V. R. Kumar, R. A. A. Muzzarelli, C. Muzzarelli, H. Sashiwa, A. J. Domb, *Chem. Rev.* **2004**, *104*, 6017-6084.

[5)] aL. Baldino, S. Concilio, S. Cardea, I. D. Marco, E. Reverchon, *J. Supercrit. Fluids* **2015**, *103*, 70-76; bS. Takeshita, S. Yoda, *Chem. Mater.* **2015**, *27*, 7569-7572.

[6)] J. Singh, P. K. Dutta, J. Dutta, A. J. Hunt, D. J. Macquarrie, J. H. Clark, *Carbohyd. Polym.* **2009**, *76*, 188-195.

[7)] M. Robitzer, A. Tourette, R. Horga, R. Valentin, M. Boissiere, J. M. Devoisselle, F. D. Renzo, F. Quinard, *Carbohyd. Polym.* **2011**, *85*, 44-53.

[8)] aJ. Wang, J.-Z. Jiang, W. Chen, Z.-W. Bai, *Carbohyd. Polym.* **2016**, *145*, 78-85; bZ.-W. Jing, Y.-Y. Jia, N. Wan, M. Luo, M.-L. Huan, T.-B. Kang, S.-Y. Zhou, B.-L. Zhang, *Biomaterials* **2016**, *84*, 276-285.

[9)] aM. S. Brody, C. A. Schalley, D. M. Rudkevich, J. Rebek, *Angew. chem. Int. Ed.*. **1999**, *38*, 1640-1644; bP. A. Gale, N. Busschaert, C. J. E. Haynes, L. E. Karagiannidis, I. L. Kirby, *Chem. Soc. Rev.* **2014**, *43*, 205-241; cD. Cornut, J. Marrot, J. Wouters, I. Jabin, *Org. Biomol. Chem.* **2011**, *9*, 6373-6384; dF. Liebner, E. Haimer, M. Wendland, M.-A. Neouze, K. Schlufter, P. Miethe, T. Heinze, A. Potthast, T. Rosenau, *Macromol. Biosci.* **2010**, *10*, 349-352.

[10)] L. Heath, L. Zhu, W. Thielemans, *ChemSusChem* **2013**, *6*, 537-544.

[11)] L. Heux, J. Brugnerotto, J. Desbrières, M.-F. Versali, M. Rinaudo, *Biomacromolecules* **2000**, *1*, 746-751.

[12)] M. Miya, R. lwamoto, S. Yoshikawa, S. Mima, *Int. J. Biol. Macromol.* **1980**, *2*, 323-324.

[13)] Y. Saito, T. Iwata, *Carbohyd. Polym.* **2012**, *87*, 2154-2159.

[14)] K. Ganesan, A. Dennstedt, A. Barowski, L. Ratke, *Mater. Des.* **2016**, *92*, 345-355.

[15)] S. Hoepfner, L. Ratke, B. Milow, *Cellulose* **2008**, *15*, 121-129.